International Journal of Innovative
Computing, Information and Control
Volume **10**, Number **3**, June **2014**

 ISSN 1349-4198
pp. **1135-1147**

ON THE SUITABILITY OF MULTISCALE IMAGE REPRESENTATION SCHEMES AS APPLIED TO NOISE REMOVAL

Epiphany Jebamalar Leavline[1], Shanmugam Sutha[2]
and Danasingh Asir Antony Gnana Singh[1]

[1]Bharathidasan Institute of Technology
Anna University
Tiruchirappalli – 24, Tamilnadu, India
{ jebilee; asirantony }@gmail.com

[2]Department of Electrical and Electronics Engineering
University College of Engineering, Panruti
Panruti – 607 106, Tamilnadu, India
suthapadmanabhan@gmail.com

Received May 2013; revised September 2013

Abstract. *The multiscale transforms extend their robust capabilities to all the fields of image processing. With the strength of the capabilities such as multiresolution, localization, critical sampling, directionality, anisotropy, sparsity, the multiscale transforms are employed and they perform well in a wide range of applications over Fourier and DCT based approaches. Image denoising is a prime part of image processing that attracts numerous researchers worldwide. Finding the better transform for denoising is considered to be a challengeable task among the researches. This paper presents a comprehensive treatise on the suitability of various multiscale image representations for denoising application. In this context, a comparability study is carried out on various aspects of the different transforms and their capabilities with their performance on image denoising in order to find the suitable transforms for denoising applications. This paper offers an insight into various multiscale image representations and their desirable features for image denoising.*

Keywords: Multiscale transforms, Image representation, Image denoising, Wavelet, Contourlet, Overcomplete, Multiscale directional filter banks

1. **Introduction.** The digital images play a key role in information and communication systems in the digital age. Visual information transmitted/received in the form of digital images are often corrupted with noise, the corrupted images must to be pre-processed before using in any applications. Denoising is the process of estimating the original image X from the observed noisy image Y. It is common to model the noise η as an additive or multiplicative component, the noisy image Y can be mathematically shown as (1) and (2) respectively.

$$Y = X + \eta \tag{1}$$

$$Y = X\eta \tag{2}$$

A good image denoising model has the significant characteristic of removing noises while preserving edge details of the image. The two major approaches followed in image denoising are namely (i) Spatial domain denoising and (ii) Transform domain denoising.

The Spatial domain denoising approach uses conventional linear filters such as Gaussian filter, Wiener filter, mean filter [1] or partial differential equation (PDE) model and nonlinear filters such as order statistic filters [2] and Total Variation (TV) filter. These filters can handle discontinuities in a much better way and preserve edges of image with minimum

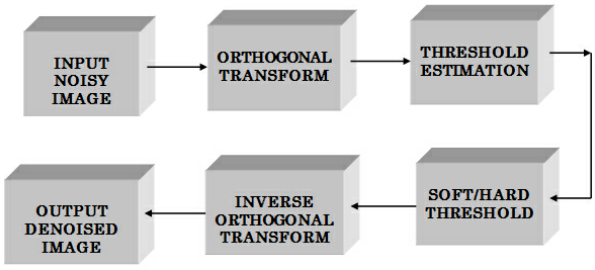

FIGURE 1. Transform domain denoising approach

computations. On the other hand, the transform domain denoising approach adopts various mathematical transforms for denoising as shown in Figure 1. These transforms perform well in image denoising with minimum computational complexity and energy compaction compared with the spatial domain approaches.

The Fourier transform successfully removes noise from the images, as it separates the various frequency components of the image. However, the major limitation of Fourier transform is that, it is not localized in time and frequency simultaneously [1].

Wavelet transform is an efficient mathematical tool for a numerous image processing applications. This mathematical tool is implemented with efficient algorithms and convenient tree data structures. Wavelet-based denoising works with the following three steps. First, an orthogonal transform is applied on the image. Then the threshold is calculated for each transformed coefficient using a non linear shrinkage functions [3]. Finally, the thresholded coefficients are reconstructed by the inverse orthogonal transform.

The literature reveals that the coefficients that correspond to noisy pixels are much smaller in magnitude than that of the clean pixels. Hence, smaller coefficients are eliminated with nonlinear shrinkage functions [3] and the image is reconstructed with the remaining coefficients.

Several wavelet-based shrinkage functions are proposed in the literature [3]. In spite of merits such as less computational complexity, multiresolution representation and high energy compaction, images denoised with wavelet based methods exhibit checkerboard artefacts. This is due to nonlocal, signal independent and fixed shaped wavelet bases. Therefore, the sharpness of the edges in the natural images is not retained with wavelet denoising. Hence, it is not a suitable denoising method for certain applications where the fine details of the images need to be preserved. This leads to the formulation of multiscale image representations that are sparse, multiresolution and highly local. Following the multiresolution properties of wavelets, a good number of multiscale image representations have been proposed in the literature. These multiscale transforms are used as efficient mathematical representations in various image processing applications such as image denoising, restoration, segmentation, compression, feature extraction and pattern recognition.

This paper presents a comprehensive study of some of the most widely used multiscale image representations that will be useful for the researchers in the field of image processing. Further, we focus on the suitability of multiscale representations for image denoising which is an essential pre-processing stage in an image processing system. Also, the attributes of multiscale image representation schemes such as Orthogonality, Basis Function, Reconstruction, Overcompleteness and computational complexity are compared to provide a fair comparison of various multiscale representations.

The rest of this paper is organized as follows. In Section 2, the importance of multiscale transforms is described. The various multiscale image representations are discussed and

analyzed in Section 3. In Section 4, the observations are presented and the features of multiscale representations are compared. Finally, the conclusion is drawn in Section 5.

2. **Importance of Multiscale Transforms.** The major limitation of wavelet transforms is its less ability to capture directional information [4]. To overcome this, multiscale and directional representations are employed to capture the intrinsic geometrical structures such as smooth contours in natural images [4-7]. These multiscale and directional representations perform scale and directional decomposition using a geometrical transform and local directional transform respectively [5].

In this context, a number of multiscale image representations are proposed in the literature that are suitable for various areas of image processing such as denoising [5,8], compression [5,9], segmentation [10], image retrieval [11], and feature extraction [12]. These multiscale representations are found suitable for a range of applications including medical imaging, remote sensing and SAR imaging [10]. Even though, most of the multiscale representations are overcomplete and have high computational complexity, they are preferred because of their ability to represent fine details of the natural images.

3. **Multiscale Image Representations for Denoising.** In this section, multiscale representations such as Gabor Wavelets, Ridgelets, Curvelets, Steerable Pyramids, Shearlets, Contourlets and multiscale directional filter banks are discussed in detail with a view to the suitability of these multiscale representations for image denoising.

3.1. **Gabor wavelets.** Gabor wavelets are developed based on the properties of the human visual system (HVS). The image enhancement and restoration applications highly make use of the Gabor functions to represent images. However, the classic Gabor expansion is carried out with unusual dual basis functions; hence, it has high computational complexity [13]. A Gabor basis function is a Gaussian function modulated with an exponential or sinusoidal function that is defined in terms of the product of a Gaussian and an exponential. The 2D Gabor function is given as (3)

$$h(x,y) = \frac{1}{2\pi\,\sigma_x\,\sigma_y}.\,e^{-\frac{1}{2}\left(\frac{x^2}{\sigma_x^2}+\frac{y^2}{\sigma_y^2}\right)}\,.\,e^{-2\pi j\,f_r\,x} \tag{3}$$

The parameters f_r, σ_x and σ_y determine the subband of Gabor filter. f_r is center frequency, σ_x and σ_y are the bandwidth of the filter [14]. Gabor functions have the following advantages [13]:

- Maximized joint localization in both spatial and frequency domains.
- Tunable to a range of spatial positions, frequencies, and orientations using arbitrary bandwidths.
- Orientation selectivity and can be expressed as a sum of only two separable filters.

Gabor functions are suitable for performing pre-processing tasks in multipurpose environments of image analysis and machine vision. However, the inverse Gabor function is computationally complex and expensive. Building a complete orthogonal basis of Gabor functions is not possible, and hence, non-orthogonal bases have to be used. Unless an overcomplete basis is considered, exact reconstruction is not possible. Also, since the Gabor wavelet is bandpass in nature, the lower and upper extreme of the frequency spectrum cannot be covered [15]. As discussed in [16], the total number of real operations required to obtain the 4×4 even channels of an $N \times N$ image [13] is approximated as in (4).

$$5\,N^2\log_2 N + 4\sum_{k=0}^{3}\binom{N}{k}^2[1+5(\log_2 N - k)] + 5\,N^2\log_2 N + N^2 \tag{4}$$

In spite of the fact that Gabor functions require complex reconstruction algorithm and do not support perfect reconstruction, the images reconstructed using Gabor wavelets are indistinguishable from the original images. The denoising performance of Gabor functions is superior to the conventional wavelet-based denoising [14].

3.2. **Ridgelet.** The wavelet based denoising is fairly difficult since the edges of the images are repeated scale after scale; and it requires a large number of wavelet coefficients to recover the edge details properly. This difficulty is overcome with the Ridgelet transform [17] and the ridgelet bases are constructed in order to provide sparse representation of both smooth functions and perfectly straight edges.

A one-dimensional wavelet transform is applied to the slices of a Radon transform in order to get the ridgelet transform [18,19]. Finally, the continuous ridgelet transforms of both smooth functions and of perfectly straight edges can be represented with adequate sparsity as per the algorithm described below [20].

Algorithm:

1. Apply the àtrous algorithm with J scales [21].
2. Apply the radon transform on detail sub-bands of J scales.
3. Calculate ridgelet coefficients by applying a one-dimensional wavelet transform on radon coefficients.
4. Get the multiscale ridgelet coefficients for J scales.

This algorithm is represented as a flow graph [20] in shown in Figure 2. An image of size $N \times N$ results in a ridgelet transform of an image of size $2N \times 2N$ [20], this introduces a redundancy factor of 4. The redundancy and over completeness of the ridgelet transform offers advantages, particularly in avoiding visual artifacts, in spite of weak critical sampling and orthogonality. However, Ridgelets have global length and variable widths exhibiting fixed anisotropy. Additionally, each step of the ridgelet transform is invertible therefore demonstrates exact reconstruction. A discrete version of the ridgelet transform is computationally efficient with $O(N^2 \log(N))$ floating point operations for an $N \times N$ image. As discussed in literature [20,22], the ridgelet transform significantly improves the visual quality and performance of denoising over wavelet denoising. The denoised images contain only a few artifacts, exhibiting high visual quality.

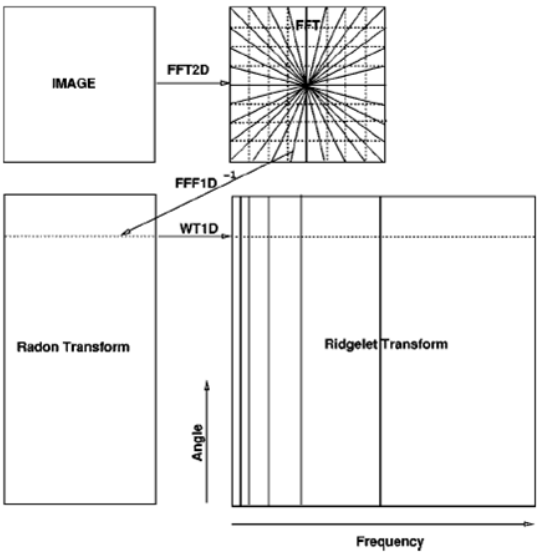

FIGURE 2. Flow graph of ridgelet transform

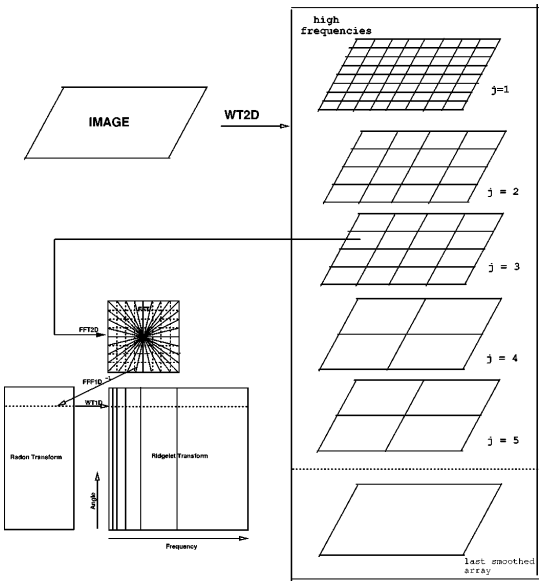

FIGURE 3. Flow graph of curvelet transform

3.3. **Curvelet.** The most important member of the multiscale family is the curvelet transform. It allows objects with edges an optimal non-adaptive sparse representation [20] by combining multiscale ridgelets with a spatial bandpass filtering operation for isolating different scales. Figure 3 depicts the curvelet decomposition that is described in the following steps [7]:

- Sub-band decomposition of the object into a sequence of sub-bands.
- Windowing each sub-band into blocks of appropriate size, depending on its center frequency.
- Applying the ridgelet transform on those blocks.

The curvelet transform has a redundancy factor of $16J + 1$ with J scales. Faster implementations of discrete curvelet transform exhibit a reduced redundancy factor of about 2.8 when wavelets are chosen at the finest scale, and 7.2 otherwise [23]. The major advantage of curvelet transforms is that exact reconstruction is possible. In addition, curvelet bases have variable anisotropy with a variable width and variable length obeying the parabolic scaling law $width \approx length^2$ [20].

The curvelet transform is much more attracted by several fields of image processing such as denoising [24,25], medical image processing [26], compression [27], retrieval, feature extraction [28], pattern recognition and the most recent application seismic data processing [29]. It works with adaptive algorithms for denoising [30] and the denoised images have very less artefacts compared with wavelet and contourlet-based denoising [20,30,31]. Still it suffers with the following limitations. Curvelets are not singly generated and rotation operations do not preserve the digital lattice used to construction of curvelet bases [32]. The curvelet construction is simple in the continuous domain rather than discrete domain since the implementation for discrete images needs to be sampled on a rectangular grid [4,5]. However, the curvelet construction demonstrates representation of images with smooth contours via a fixed transform to remove the noise from the images with very less artefacts [20].

3.4. **Shearlet.** Shearlet is another category of multiscale transform [33], able to sparsely represent anisotropic features by optimal encoding of several classes of multivariate data. In contradiction to curvelets, shearlets use shearing to control the directional selectivity. A single or finite set of generators develop the Shearlet system ensuring a unified handling of the continuum and digital world since the shear matrix reserves the integer lattice. The elements of Shearlet representation are listed below [34]:

- A single or a finite set of generating functions
- Optimally sparse approximations of anisotropic features in multivariate data
- Compactly supported analyzing elements
- Fast algorithmic implementations
- A unified treatment of the continuum and digital realms
- Association with classical approximation spaces

The compactly supported shearlets achieve directionality and excellent spatial localization [35]. They are tight frames hence requires iterative methods for synthesis process yet possess the property of stable reconstruction [34].

The trade-off among compact support of Shearlet generators, tight frames and separability of the Shearlet generators is also considered [36]. The frequency support of the Shearlet satisfies parabolic scaling. There is no restriction on the number of directions and the size of the supports for shearing, unlike the construction of the directional filter banks in contourlet transforms [37]. The inversion of the discrete Shearlet transform is formed by summing all the shearing filters rather than inverting a directional filter bank.

The Shearlet transform denoise the images with very less Gibbs-type residual when the shearing filters of small support sizes are used [37]. An overcomplete decomposition of the image is introduced to prevent the blocking artefacts, and then synthesized by a lapped window scheme [20].

The Shearlet decomposition is significantly redundant, because the down-sampling is applied only in the vertical and horizontal directions with no anisotropic sub-sampling. Given an image of size $N \times N$, three-level decomposition would result in $2^j N^2 + 2^{j-1}(N/4)^2 + (N/16)^2$ coefficients when 2^j directional subbands are chosen at the first decomposition level [37].

As stated in [35], the discrete Shearlet transform has a redundancy ratio less than or equal 2, and shows significant improvement in redundancy ratio with $O(N^2 \log N)$ computations. The Shearlet approach can also be extended to multidimensional and multiresolution analysis too [38].

3.5. **Steerable pyramid.** The steerable pyramid is a multi-scale, multi-directional representation similar to a two-dimensional discrete wavelet transform with directional subbands of the image. Critically sampled translation-variant schemes such as wavelets suffer with instability and aliasing in the presence of noise. Steerable pyramids deal this issue using a rotation and translation invariant overcomplete basis that is optimized for increased orientation selectivity [39]. As proved by Raphan and Simoncelli, this representation is overcomplete by a factor of $4K/3+1$, where K is the number of orientation bands utilized [40]. However, the overcompleteness is very useful in image analysis. Translations and rotations of a single function are the basis filters of the steerable pyramid. The filter at any orientation can be computed as a linear combination of the basis filters [41]. Figure 4 shows the decomposition scheme of the steerable pyramid. The image is decomposed into low-pass and high-pass subbands and decomposition is iterated in the lowpass subband [42].

Natural images contain oriented or elongated structures (such as lines, edges, and textures), while noise components do not possess any preferred orientation. Hence, an image representation based on steerable pyramid easily determines whether the structure is due to noise or image. So, the steerable pyramid can be effectively used for image enhancement and restoration as it tends to preserve the contents of the image representation that correspond to visually significant oriented structures in the image [39].

3.6. **Bandelet.** Wavelet bases exploit only the isotropic regularity of square domains of varying sizes. However, the geometric regularity in images along edges exhibits an anisotropic regularity. The bandelet transform exploits anisotropic regularity in images by constructing orthogonal vectors that are elongated in the direction of maximum regularity. Critically sampled orthogonal bandelet bases are obtained from a wavelet basis with an additional cascade of orthogonal operators parameterized by the local geometry of the image [43].

Bandelet decomposition is derived with a wavelet filter bank followed by directional orthogonal filters. Each geometric direction leads to a different transform, and the optimal set of filters can be found using the best basis algorithm [44]. The bandelet bases are obtained with a bandeletization of warped wavelet bases, which takes advantage of the image regularity along the geometric flow. Orthogonal bandelet bases are constructed by dividing the image support in regions inside which the geometric flow is parallel.

A fast discrete bandelet (FDB) transform was introduced in [6] that is computed from a fast separable wavelet transform along a fixed direction and along the image flow lines. The image partitioning associated with the FDB transform has three phases:

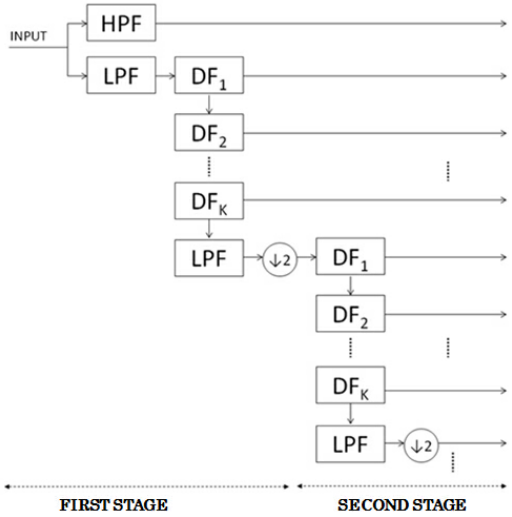

FIGURE 4. Steerable pyramid decomposition

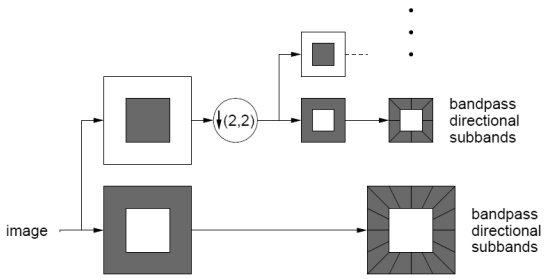

FIGURE 5. Iterative double filter bank structure for contourlet transform

- A resampling, that computes the image sample values along the flow lines in each region of the partition;
- A warped wavelet transform with a subband filtering along the flow lines, which goes across the region boundaries;
- A bandletization that transforms the warped wavelet coefficient to compute bandlet coefficients along the flow lines.

The fast inverse bandlet transform includes the three inverse steps:

- An inverse bandletization that recovers the warped wavelet coefficient along the flow lines;
- An inverse warped wavelet transform with an inverse subband filtering;
- An inverse resampling which computes image samples along the original grid from the samples along the flow lines in each region using fast algorithms that implement these three steps, with $O(n^2)$ operations for an image of 'N' pixels.

The direct reconstruction of an image from its bandelet coefficients leads to blocking effects. Alternatively, the reconstruction can be performed with the classical iterative frame algorithm on the full bandlet frame, which avoids the blocking effect but requires an iterative reconstruction algorithm. Also, a bandlet lifting scheme has been proposed that removes the blocking effects [45]. The bandlet estimator outperforms the wavelet estimator for image compression and denoising. The quantitative results of [6,46] show that optimized bandlet bases improve significantly over wavelet bases.

3.7. **Contourlet.** The conventional wavelet transforms are separable and fail to exploit all the directional information in natural images because of its limited directional selectivity. Contourlet transforms overcome this by introducing basis functions which are local, directional, and with multiresolution expansion.

First, a wavelet-like multiscale transform is applied, and then a local directional transform is used to gather the nearby basis functions at the same scale into linear structures. This representation has two basic building blocks, the Laplacian pyramid (LP) and the Directional Filter Bank (DFB).

A computationally efficient iterative double filter bank structure (Figure 5) proposed in [4,5] uses Laplacian pyramid [46] to capture the point discontinuities, followed by a directional filter bank [47] to connect point discontinuities into linear structures. Contourlets can efficiently approximate a smooth contour at multiple resolutions since they have elongated bases at various scales, directions, and aspect ratios. The discrete contourlet transform achieves perfect reconstruction if the LP and DFB use perfect reconstruction filters with redundancy ratio of 4/3 [5]. Contourlet frames are compactly supported with flexible anisotropy that follows $width \approx length^2$.

According to Cheng et al., if M is the length of the FIR filter, N is the number of pixels and L_d is the levels of decomposition in DFB, the number of computations involved in a contourlet transform is approximated to $\left(\frac{16}{3} + \frac{8}{3} L_d\right) MN$, where the first term is from the pyramidal filter and the second is from the directional filter [48].

Random noise will generate only a few significant contourlet coefficients unlike wavelet representation. Significant denoising performance is achieved with simple shrinkage methods on contourlet coefficients [4]. The contourlet transform is shown to be more effective in recovering smooth contours, both visually as well as in terms of Peak Signal-to-Noise Ratio (PSNR) [49].

3.8. **Multiscale Directional Filter Banks (MDFBs) and Fast Multiscale Directional Filter Banks (FMDFBs).** Pyramidal directional filter banks (PDFBs) or contourlet transforms, detailed in Section 3.7 are computationally efficient while providing a high angular resolution. In [50], a modification to the PDFB was proposed, namely the multiscale directional filter bank (MDFB) which has fine high-frequency decomposition. Similar to Contourlets, in MDFB the LP and the DFB are combined in order to support the multiscale property. The MDFB is redundant and a number of possible structures are available based on the choice of lowpass filter and the number of directional decomposition, as in the one detailed in [50]. The major advantage of MDFB is that the bandpass images derived from MDFB decomposition do not suffer from aliasing [48]. According to Cheng et al. [48], MDFB introduces an additional decomposition in the high-frequency band and thereby improves the radial frequency resolution at a cost of one set of extra scale and directional decompositions on the full image size. This result in an increased number of computations, approximately $\left(\frac{22}{3} + \frac{14}{3} L_d\right) MN$. In addition, MDFB has a higher redundancy than contourlet transforms. The over completeness and increased frequency resolution of MDFB was found useful in applications like texture characterization and retrieval [48,50].

Cheng et al. in [51,52] proposed a fast and reduced redundancy structure for MDFB (FMDFB), shown in Figure 6. The idea behind achieving reduced redundancy and computational complexity is that, directional decomposition on the first two scales is performed prior to the scale decomposition. This allows sharing of directional decomposition among the two scales, thus reducing the computational complexity significantly. The resultant scheme has the same redundancy as a contourlet transform and almost 33% reduction in number of computations as compared with MDFB. FMDFB exhibits perfect reconstruction irrespective of the choice of low pass filters. Since the directional decomposition with lower angular resolution is performed before scale decomposition one set of operations for directional decomposition with lower angular resolution is saved by sharing [51].

The total number of subband coefficients is the same as the size of the original image because of the critically sampled DFB, and hence no extra computations are introduced by the scale decomposition. The computational complexity of FMDFB [52] is approximated as $\left(\frac{19}{3} + \frac{8}{3} L_d\right) MN$. In [8] we have introduced a multiscale denoising approach using FMDFB for additive gaussian noise removal. Also, from our previous work [53,54], it

is evident that denoising scheme using FMDFB yield better results than wavelet and contourlet approaches both visually and in terms of PSNR. Moreover, it preserves fine details such as edges when compared with wavelet and contourlet based denoising methods [8,53].

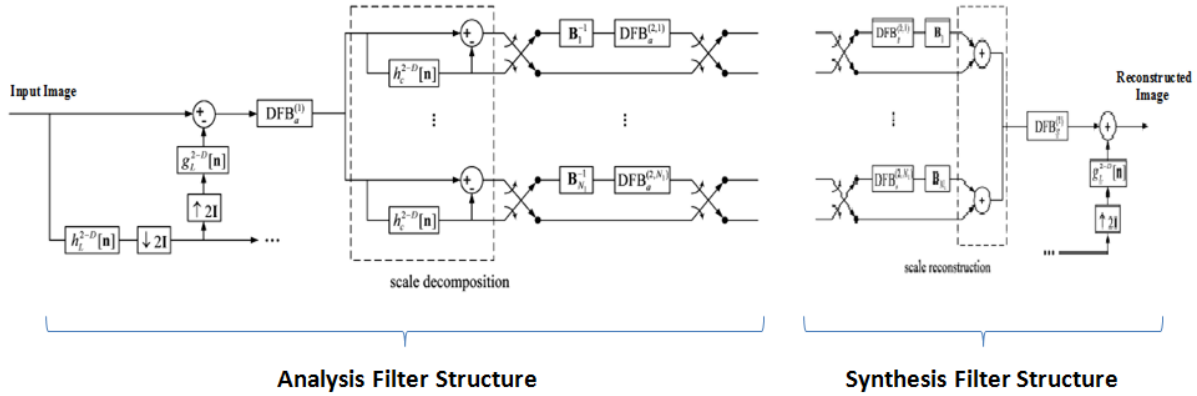

FIGURE 6. Analysis and synthesis filter bank structure for FMDFB. h_L and g_L are the lowpass and highpass filters respectively in LP. B_i and B_i^{-1} represent the back sampling and inverse back sampling. DFB is the directional filter bank for direction decomposition.

4. **Observations and Discussion.** Each of the multiscale image representations discussed has distinct characteristics and their own pros and cons. Wavelets were the best tool for denoising until recently because of lower computational complexity and effective multiresolution structures. Nevertheless, the denoised images have some checkerboard artefacts, mainly due to the square basis functions. Wavelets lack in directionality, which is a key characteristic in natural images. Hence, wavelets fail in situations where the image details are very important. Multiscale image representations are a better choice in applications where fine details such as edges, contours and textures need to be preserved. Almost all multiscale transforms are overcomplete with a significant redundancy ratio. Yet, some schemes like bandlets and FMDFB are quite appealing because of their maximally decimated (critical sampling) property. However, representations such as Gabor wavelets and bandlets do not support perfect reconstruction and hence the overall reconstruction is lossy in nature. Anisotropy is another important feature as far as multiscale representations are concerned, and most of them follow the parabolic scaling law. A comparison of the salient features of various multiscale transforms is shown in Table 1.

From the image denoising perspective, the need for a multiscale, multiresolution and sparse image representation that can preserve image details continues to grow. Multiscale transforms, discussed in Section 3, have been used for image denoising in the literature. Gabor wavelets perform better than conventional wavelets, but require complex reconstruction algorithm and do not support perfect reconstruction. Ridgelets, curvelets, shearlets and bandlets show some artefacts in the denoised images. Steerable pyramids can be effectively used for image enhancement and restoration since they preserve the details of the image that correspond to visually significant oriented structures in the image. Yet, the redundancy ratio increases linearly with the number of orientation banks which is undesirable.

In spite of a redundancy ratio of 1.33, contourlet transforms are shown to be more effective in recovering smooth contours in images, both visually as well as in terms of PSNR. The key advantage of contourlet-based denoising is that simple thresholding schemes can

TABLE 1. Comparison of salient features (Orthogonality, Basis function, Reconstruction, Overcompleteness and Computational complexity) of various multiscale transforms. Unless specified, J is the level of decomposition, K is the number of orientation bands, N is the number of image pixels, and M is the length of the FIR filters.

Multiscale representation /Characteristics	Orthogonality	Basis function	Reconstruction	Over completeness	Computation complexity
Wavelet	Orthogonal	Square	Perfect	1 (Critically sampled)	$O(N)$
Gabor Wavelet	Non-orthogonal	Gaussian	Not exact	overcomplete	$O(N \log N)$
Ridgelet	Weakly orthogonal	Fixed anisotropy	Perfect	4	$O(N^2 \log(N))$
Curvelet	Near orthogonal	Variable anisotropy	Perfect	$16J + 1$ 7.8 (Fast curvelet)	$O(N^2 \log N)$ for $N \times N$ image
Shearlet	Orthogonal	Parabolic scaling	Stable	2	$O(N^2 \log N)$
Steerable Pyramid	Non-orthogonal	Gaussian	Perfect	$4K/3 + 1$	$O(N \log N)$
Bandelets	Orthogonal	Elongated shape	Small approximation error	1 (Critically sampled)	$O(N^{3/2})$ to $O(N)$
Contourlet	Orthogonal	Elongated shape	Perfect	1.33	$\left(\frac{16}{3} + \frac{8}{3} L_d\right) MN$
MDFB	Orthogonal	Elongated shape	Perfect	1.33	$\left(\frac{22}{3} + \frac{14}{3} L_d\right) MN$
FMDFB	Orthogonal	Elongated shape	Perfect	1 (Critically sampled)	$\left(\frac{19}{3} + \frac{8}{3} L_d\right) MN$

be applied on contourlet coefficients. Even though better frequency resolution is achieved at the cost of increased computational complexity, the denoising performance of MDFB is similar to that of the contourlet transform.

FMDFB is better than multiscale transforms discussed in terms of overcompleteness and computational complexity. It is an orthogonal scheme with elongated shaped support and the reconstruction is perfect irrespective of the filters used. As evident from [8,53], FMDFB outperforms conventional wavelet- and contourlet-based denoising, both visually and in terms of PSNR. However, large number of FMDFB subbands at finer decomposition scales would complicate the denoising process and FMDFB can be applied only for square images of dyadic size (integer power of two).

5. **Conclusion.** Multiscale image representations such as Gabor wavelets, ridgelets, curvelets, steerable pyramids, shearlets, Contourlets and multiscale directional filter banks are discussed in this paper with a focus on image denoising. Also, the features of these transforms, such as orthogonality, basis function, reconstruction, overcompleteness and computational complexity are analyzed. Each of the representations discussed possess their own merits and demerits. The tradeoff between several features of these multiscale representations can be considered before choosing a multiscale representation for a particular application. In image denoising point of view, the representations that can preserve fine details such as edges would be preferred since the fine details describe the essential features that are required for applications such as image analysis. In addition, the computational complexity can also be taken into account as it aids for real time implementations of image processing and analysis algorithms.

Acknowledgment. The authors gratefully acknowledge the helpful comments and suggestions of the reviewers, which have improved the presentation.

REFERENCES

[1] R. C. Gonzalez and E. Richard, *Digital Image Processing*, 2002.
[2] E. Jebamalar Leavline and D. Asir Anton Gnana Singh, Enhanced modified decision based unsymmetric trimmed median filter for salt and pepper noise removal, *International Journal of Imaging & Robotics*, vol.11, no.3, pp.46-56, 2013.
[3] E. J. Leavline, S. Sutha and D. A. A. Gnana, Wavelet domain shrinkage methods for noise removal in images: A compendium, *International Journal of Computer Applications*, vol.33, no.10, 2011.
[4] D.-Y. Po and M. N. Do, Directional multiscale modeling of images using the contourlet transform, *IEEE Transactions on Image Processing*, vol.15, no.6, pp.1610-1620, 2006.
[5] M. N. Do and M. Vetterli, The contourlet transform: An efficient directional multiresolution image representation, *IEEE Transactions on Image Processing*, vol.14, no.12, pp.2091-2106, 2005.
[6] E. Le Pennec and S. Mallat, Sparse geometric image representations with bandelets, *IEEE Transactions on Image Processing*, vol.14, no.4, pp.423-438, 2005.
[7] M. N. Do and M. Vetterli, Pyramidal directional filter banks and curvelets, *Proc. of International Conference on Image Processing*, vol.3, pp.158-161, 2001.
[8] E. J. Leavline and S. Sutha, Gaussian noise removal in gray scale images using fast multiscale directional filter banks, *International Conference on Recent Trends in Information Technology*, pp.884-889, 2011.
[9] M. N. Do and M. Vetterli, Orthonormal finite ridgelet transform for image compression, *Proc. of International Conference on Image Processing*, vol.2, pp.367-370, 2000.
[10] Y. Li and M. He, Texture-based segmentation of high resolution SAR images using contourlet transform and mean shift, *IEEE International Conference on Information Acquisition*, pp.201-206, 2006.
[11] Y. D. Chun, N. C. Kim and I. H. Jang, Content-based image retrieval using multiresolution color and texture features, *IEEE Transactions on Multimedia*, vol.10, no.6, pp.1073-1084, 2008.
[12] M. Nabti and A. Bouridane, An effective and fast iris recognition system based on a combined multiscale feature extraction technique, *Pattern Recognition*, vol.41, no.3, pp.868-879, 2008.
[13] O. Nestares, R. Navarro, J. Portilla and A. Tabernero, Efficient spatial-domain implementation of a multiscale image representation based on gabor functions, *Journal of Electronic Imaging*, vol.7, no.1, pp.166-173, 1998.
[14] N. Nezamoddini-Kachouie and P. Fieguth, A Gabor based technique for image denoising, *Canadian Conference on Electrical and Computer Engineering*, pp.980-983, 2005.
[15] S. Fischer, F. Šroubek, L. Perrinet, R. Redondo and G. Cristóbal, Self-invertible 2D log-Gabor wavelets, *International Journal of Computer Vision*, vol.75, no.2, pp.231-246, 2007.
[16] A. B. Watson, The cortex transform: Rapid computation of simulated neural images, *Computer Vision, Graphics, and Image Processing*, vol.39, no.3, pp.311-327, 1987.
[17] M. N. Do and M. Vetterli, The finite ridgelet transform for image representation, *IEEE Transactions on Image Processing*, vol.12, no.1, pp.16-28, 2003.
[18] P. Goel, H. P. Sinha and H. Singh, Ultrasound image denoising using multiscale ridgelet transform with hard and NeighCoeff thresholding – Google search, *International Journal of Computer & Communication Technology*, vol.2, no.7, pp.65-70, 2011.
[19] R. N. Bracewell, Numerical transforms, *Science*, vol.248, no.4956, pp.697-704, 1990.
[20] J.-L. Starck, E. J. Candès and D. L. Donoho, The curvelet transform for image denoising, *IEEE Transactions on Image Processing*, vol.11, no.6, pp.670-684, 2002.
[21] Y.-B. Xu, C.-S. Xie and C.-Y. Zheng, An application of the a trous algorithm in detecting infrared targets, *International Conference on Wavelet Analysis and Pattern Recognition*, vol.3, pp.1015-1019, 2007.
[22] G. Y. Chen and B. Kégl, Image denoising with complex ridgelets, *Pattern Recognition*, vol.40, no.2, pp.578-585, 2007.
[23] E. Candès, L. Demanet, D. Donoho and L. Ying, Fast discrete curvelet transforms, *Multiscale Modeling & Simulation (Society for Industrial and Applied Mathematics)*, vol.5, no.3, pp.861-899, 2006.
[24] A. A. Patil and J. Singhai, Image denoising using curvelet transform: An approach for edge preservation, *Journal of Scientific and Industrial Research*, vol.69, no.1, pp.34-38, 2010.
[25] S. Palakkal and K. M. M. Prabhu, Poisson image denoising using fast discrete curvelet transform and wave atom, *Signal Processing*, vol.92, no.9, pp.2002-2017, 2012.

[26] M. A. Hamdi, A comparative study in wavelets, curvelets and contourlets as denoising biomedical images, *Image Processing & Communications*, vol.16, no.3, pp.13-20, 2011.
[27] Y. Li, Q. Yang and R. Jiao, Image compression scheme based on curvelet transform and support vector machine, *Expert Systems with Applications*, vol.37, no.4, pp.3063-3069, 2010.
[28] X. Jiang, W. Zeng, P. Scott, J. Ma and L. Blunt, Linear feature extraction based on complex ridgelet transform, *Wear*, vol.264, no.5, pp.428-433, 2008.
[29] G. Tang and J. Ma, Application of total-variation-based curvelet shrinkage for three-dimensional seismic data denoising, *Geoscience and Remote Sensing Letters, IEEE*, vol.8, no.1, pp.103-107, 2011.
[30] A. A. Youssif, A. A. Darwish and A. M. M. Madbouly, Adaptive algorithm for image denoising based on curvelet threshold, *International Journal of Computer Science and Network Security*, vol.10, no.1, pp.322-328, 2010.
[31] M. Goyal and S. Kaur, Comparative analysis of filters with curvelet transform for denoising in ultrasound images, *International Journal of Computer Science & Technology*, vol.2, no.4, pp.190-194, 2011.
[32] K. Guo and D. Labate, The construction of smooth Parseval frames of shearlets, *Mathematical Modelling of Natural Phenomena*, vol.8, no.1, pp.82-105, 2013.
[33] G. Kutyniok, M. Shahram and X. Zhuang, Shearlab: A rational design of a digital parabolic scaling algorithm, *SIAM Journal on Imaging Sciences*, vol.5, no.4, pp.1291-1332, 2012.
[34] G. Kutyniok and D. Labate, Introduction to shearlets, in *Shearlets*, Springer, 2012.
[35] W.-Q. Lim, The discrete shearlet transform: A new directional transform and compactly supported shearlet frames, *IEEE Transactions on Image Processing*, vol.19, no.5, pp.1166-1180, 2010.
[36] G. Kutyniok, J. Lemvig and W.-Q. Lim, Compactly supported shearlets, in *Approximation Theory XIII: San Antonio 2010*, Springer, 2012.
[37] G. Easley, D. Labate and W.-Q. Lim, Sparse directional image representations using the discrete shearlet transform, *Applied and Computational Harmonic Analysis*, vol.25, no.1, pp.25-46, 2008.
[38] B. Han, G. Kutyniok and Z. Shen, Adaptive multiresolution analysis structures and shearlet systems, *SIAM Journal on Numerical Analysis*, vol.49, no.5, pp.1921-1946, 2011.
[39] E. P. Simoncelli, W. T. Freeman, E. H. Adelson and D. J. Heeger, Shiftable multiscale transforms, *IEEE Transactions on Information Theory*, vol.38, no.2, pp.587-607, 1992.
[40] M. Raphan and E. P. Simoncelli, Optimal denoising in redundant representations, *IEEE Transactions on Image Processing*, vol.17, no.8, pp.1342-1352, 2008.
[41] A. P. Vo, S. Oraintara and T. T. Nguyen, Using phase and magnitude information of the complex directional filter bank for texture image retrieval, *IEEE International Conference on Image Processing*, vol.4, pp.61-64, 2007.
[42] H. Rabbani, Image denoising in steerable pyramid domain based on a local Laplace prior, *Pattern Recognition*, vol.42, no.9, pp.2181-2193, 2009.
[43] S. Mallat and G. Peyré, A review of bandlet methods for geometrical image representation, *Numerical Algorithms*, vol.44, no.3, pp.205-234, 2007.
[44] G. Peyré and S. Mallat, Discrete bandelets with geometric orthogonal filters, *Proc. of IEEE International Conference on Image Processing*, vol.1, pp.65-68, 2005.
[45] E. Le Pennec and S. Mallat, Bandelet image approximation and compression, *Multiscale Modeling & Simulation*, vol.4, no.3, pp.992-1039, 2005.
[46] P. Burt and E. Adelson, The Laplacian pyramid as a compact image code, *IEEE Transactions on Communications*, vol.31, no.4, pp.532-540, 1983.
[47] R. H. Bamberger and M. J. Smith, A filter bank for the directional decomposition of images: Theory and design, *IEEE Transactions on Signal Processing*, vol.40, no.4, pp.882-893, 1992.
[48] K.-O. Cheng, N.-F. Law and W.-C. Siu, Multiscale directional filter bank with applications to structured and random texture retrieval, *Pattern Recognition*, vol.40, no.4, pp.1182-1194, 2007.
[49] Z.-F. Zhou and P.-L. Shui, Contourlet-based image denoising algorithm using directional windows, *Electronics Letters*, vol.43, no.2, pp.92-93, 2007.
[50] W. Y. Chan, N. F. Law and W. C. Siu, Multiscale feature analysis using directional filter bank, *Proc. of the 2003 Joint Conference of the 4th International Conference on Information, Communications and Signal Processing, 2003 and the 4th Pacific Rim Conference on Multimedia*, vol.2, pp.822-826, 2003.
[51] K. O. Cheng, N. F. Law and W. C. Siu, A novel fast and reduced redundancy structure for multiscale directional filter banks, *IEEE Transactions on Image Processing*, vol.16, no.8, pp.2058-2068, 2007.
[52] K. O. Cheng, N. F. Law and W. C. Siu, Fast multiscale directional filter bank with applications to texture retrieval, *Pattern Recognition*, 2007.

[53] S. Sutha, E. Jebamalar Leavline and D. Asir Antony Gnana Singh, A novel denoising algorithm using fast multiscale directional filter banks, *European Jour. Sci. Res.*, vol.86, no.4, pp.493-501, 2012.

[54] S. Sutha, E. Jebamalar Leavline and D. Asir Antony Gnana Singh, IHNS: A pragmatic investigation on identifying highly noisy subband in FMDFB for fixing threshold to deteriorate noise in images, *Information Technology Journal*, vol.12, no.7, pp.1289-1298, 2013.